
Critical Behavior of Electron Impact Ionization of Atoms

IMAD LADADWA,^{1,2} SABRE KAIS¹

¹*Department of Chemistry, Purdue University, West Lafayette, Indiana 47907*

²*Department of Physics, University of Bergen, Allegaten 55, N-5007 Bergen, Norway*

Received 11 April 2000; accepted 20 June 2000

ABSTRACT: Cross sections of the electron impact ionization for different atoms are calculated numerically in the Born approximation as a function of both the incident electron energy and the nuclear charge Z of the ionized atom. We show that the cross section for ionization tends to a large magnitude as the nuclear charge of the target atom tends to its critical value, where the critical nuclear charge is the minimum charge necessary to bind N electrons. Results show that there is a fundamental difference in the change of the cross section near the critical point depending on whether the transition from bound to a continuum state is first order or continuous. The cross section for ionization and the threshold power law for two and three electrons are discussed.

© 2000 John Wiley & Sons, Inc. Int J Quantum Chem 80: 575–581, 2000

Key words: cross section; electron impact ionization; critical point; phase transition

Introduction

The problem of stability of a given quantum system of charged particles is of fundamental importance in atomic and molecular physics. When the charge of one of the particles varies, the system might go from stable to metastable or to unstable configurations. Therefore, it is important, for example, to calculate the critical nuclear charge for a given atom, the minimum charge necessary to bind N -electrons. For the two-electron atoms with the configuration $1s^2$, the critical charge was found to

be $Z_c \simeq 0.911$. The fact that this critical charge is below $Z = 1$ explains why H^- is a stable negative ion [1]. While for the three-electron atoms, the critical nuclear charge for the ground state was found to be $Z_c \simeq 2$, which explains why the He^- and He^{-2} are unstable negative ions [2].

Recently [3, 4] we have found that one can describe stability of atomic ions and symmetry breaking of electronic structure configurations as quantum phase transitions and critical phenomena. This analogy was revealed [3] by using the large dimensional limit model of electronic structure configurations [5]. Quantum phase transitions can take place as some parameter in the Hamiltonian of the system is varied. For the Hamiltonian of N -electron atoms, this parameter is taken to be the nuclear charge. As the nuclear charge reaches a critical point, the quan-

Correspondence to: S. Kais; e-mail: kais@power1.chem.purdue.edu.

Contract grant sponsor: NSF Early-Career Award.

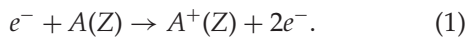
tum ground state changes its character from being bound to being degenerate or absorbed by a continuum. For larger atoms, we have developed a simple one-particle model to estimate the nuclear critical charge for any N -electron atom. This model has one free parameter, which was fitted to meet the known binding energy of the neutral atom and its isoelectronic negative ion. The critical charges are found for atoms up to Rn ($N = 86$) [6]. This study will attempt to extend this analogy of phase transitions to the scattering states.

Here we use the one-particle model, which is very accurate near the critical nuclear charge, along with the Born approximation to investigate the change of the electron impact ionization cross section as a function of the atomic nuclear charge. In the following section we review the Born approximation for the calculation of electron impact ionization cross section. The third section gives the one-particle model used to approximate the interaction between a loosely bound electron and the atomic core in a multielectron atom. The calculated cross section as a function of both the incident electron energy and the nuclear charge for two-, three-, and nine-electron atoms is given in the fourth section. Finally, we discuss the effect of the order of the phase transitions, first order or continuous, on the ionization cross section as a function of the nuclear charge.

Electron Impact Ionization of Atoms

There are many different methods for the calculations of the electron impact ionization cross section for different elements. These calculations included ionization of neutral atoms as well as detachment of negative ions by electron impact. These methods include the convergent close coupling (CCC) methods [7], the R -matrix methods [8, 9], classical phenomenological techniques [10], fully quantum methods [11, 12], and semiclassical methods [13, 14].

In this study we will use the Born approximation for the evaluation of the ionization cross sections as a function of the atomic nuclear charge. We expect the Born approximation to be a good approximation near the critical nuclear charge since the outermost electron is loosely bound. We will consider mainly the electron impact ionization of an atom A with a continuously variable nuclear charge Z :



In the Born approximation, the scattering amplitude for an incident electron and an atom is given

by

$$f_B = -\frac{1}{2\pi} \langle \psi_{\mathbf{k}_f} | V | \psi_{\mathbf{k}_i} \rangle, \quad (2)$$

where \mathbf{k}_i and \mathbf{k}_f are the momenta of the incident electron before and after the collision, respectively. The matrix element is that of the energy of interaction between the incident electron and the atom:

$$V(\mathbf{r}, \mathbf{R}) = -\frac{Z}{R} + \frac{1}{|\mathbf{R} - \mathbf{r}'|}, \quad (3)$$

where \mathbf{R} is the radius vector of the incident electron, \mathbf{r} is of the atomic electron, the origin of the coordinate system is at the nucleus of the atom. The wave functions for initial and final states are given by

$$\psi_{\mathbf{k}_i} = e^{i\mathbf{k}_i \cdot \mathbf{R}} \phi_i(\mathbf{r}), \quad (4)$$

$$\psi_{\mathbf{k}_f} = e^{i\mathbf{k}_f \cdot \mathbf{R}} \phi_f(\mathbf{r}). \quad (5)$$

Integrating over \mathbf{R} reduces the scattering amplitude to the form

$$f_B = \frac{2}{K^2} \langle \phi_f(\mathbf{r}) | e^{i\mathbf{K} \cdot \mathbf{r}} | \phi_i(\mathbf{r}) \rangle, \quad (6)$$

where $\mathbf{K} = \mathbf{k}_f - \mathbf{k}_i$ is the momentum transfer during the collision.

The scattering amplitude in Born approximation can be further simplified by using the multipole expansion of the expression $e^{i\mathbf{K} \cdot \mathbf{r}}$ as

$$e^{i\mathbf{K} \cdot \mathbf{r}} = 4\pi \sum_{LM} i^L j_L(Kr) Y_{LM}^*(\hat{K}) Y_{LM}(\hat{r}), \quad (7)$$

where j_L is the spherical Bessel function and Y_{LM} is a spherical harmonic. This leads to the following form for the scattering amplitude:

$$f_B = \frac{2}{K^2} V_{fi}, \quad (8)$$

where

$$V_{fi} = \left\langle \phi_f(\mathbf{r}) \left| 4\pi \sum_{LM} i^L j_L(Kr) Y_{LM}^*(\hat{K}) Y_{LM}(\hat{r}) \right| \phi_i(\mathbf{r}) \right\rangle. \quad (9)$$

Substituting the explicit form of the initial and final wave functions and integrating over the volume element $r^2 dr d\Omega$ gives

$$V_{fi} = \sum_{LM} i^L 4\pi [F_{El_f, n_i l_i}^L(K)] [C^L] [Y_{LM}^*(\hat{K})], \quad (10)$$

where

$$F_{El_f, n_i l_i}^L(K) = \int_0^\infty dr r^2 R_{n_i l_i}(r) R_{El_f}^*(r) j_L(Kr), \quad (11)$$

where $R_{n_i l_i}$ and R_{El_f} are the initial and final radial wave functions. These F functions are evaluated in Ref. [15], while R_{El_f} , the continuum wave function

for the released electron, is given in Ref. [16], these continuum wave functions are calculated here numerically using the model potential V_{mod} given in the next section by Eq. (14), and C^L is the integration of three spherical harmonics given by

$$C^L = \int Y_{l_f m_f}^*(\hat{r}) Y_{LM}(\hat{r}) Y_{l_i m_i}(\hat{r}) d\Omega$$

$$= (-1)^{m_f} \left[\frac{(2l_f + 1)(2L + 1)(2l_i + 1)}{4\pi} \right]^{1/2}$$

$$\times \begin{pmatrix} l_f & L & l_i \\ -m_f & M & m_i \end{pmatrix} \begin{pmatrix} l_f & L & l_i \\ 0 & 0 & 0 \end{pmatrix}. \quad (12)$$

The integral is different from zero if $m_f = M + m_i$ and $l_f + L + l_i$ is even.

The quantities denoted by $\begin{pmatrix} a & b & c \\ d & e & f \end{pmatrix}$ are the Wigner 3j-symbols.

Finally, the electron impact ionization cross section can be evaluated using the calculated scattering amplitude f_B :

$$\sigma = \frac{k_f}{k_i} \int |f_B(\theta, \phi)|^2 d\Omega, \quad (13)$$

where $d\Omega$ is an element of the solid angle.

One-Particle Model

The present study deals with the electron impact ionization of a multielectron atom considered as a function of the nuclear charge. For the movement of a loosely bound valence electron, we have developed a simple one particle potential based on the reliable data for the ionization energy of a negative ion and a neutral atom, which were calculated or experimentally measured [6]. This model is realistic in the vicinity of the critical charge, the minimum charge necessary to bind N electrons, and effectively reproduces the nontrivial singularity of the ionization energy at the critical charge. The results for the critical charges agree (within an accuracy of 0.01) with both the ab initio multireference configuration interaction calculations of Hogreve [17] and the critical charges extracted from Davidson's figures of isoelectronic energies [18].

For a given atom with N electrons and a nuclear charge Z , the potential of interaction, in atomic units, between the loose electron and an atomic core consisting of the nucleus and the other $N - 1$ electrons tends to $-Z/r$ at small r and to $(-Z + N - 1)/r$ at large r . After the scaling transformation $r \rightarrow Zr$, the model potential with two parameters γ and δ

takes the form

$$V_{\text{mod}}(r) = -\frac{1}{r} + \frac{\gamma}{r}(1 - e^{-\delta r}). \quad (14)$$

In these scaled units, the potential of interaction between a valence electron and a core tends to $-1/r$ at small r and tends to $(-1 + \gamma)/r$ with $\gamma = (N - 1)/Z$ at large r . It is easy to see that the model (14) correctly reproduces such an effective potential both at small r and at large r . The transition region between $-1/r$ behavior and $(-1 + \gamma)/r$ behavior has the size of the core that is about $1/\delta$ [6].

The second parameter of the model potential, δ , is chosen to make the binding energy $-E$ in the potential, Eq. (14), be equal to the ionization energy of an atom (or an ion). In our previous study [6], we have shown that the behavior of the function $\delta(\gamma)$ near $\gamma = 1$ that corresponds to $Z = N - 1$ can be approximated by

$$\delta = \frac{\delta_0(\gamma - \gamma_1) - \delta_1(\gamma - \gamma_0)}{\gamma_0 - \gamma_1}, \quad (15)$$

where $\gamma_0 = (N - 1)/N$, δ_0 are parameters corresponding to the neutral atom and $\gamma_1 = 1$, δ_1 are parameters corresponding to the isoelectronic negative ion. Ionization energy E_I is calculated by solving the Schrödinger equation with the potential (14) at $\gamma = (N - 1)/Z$ and δ determined by Eq. (15). Results of fitting the parameter δ for elements with $N \leq 86$ is given in our previous study [6]. The parameters (γ, δ) used in this study are given in Table I.

Results and Discussion

Using the Born approximation as described above, we calculated the ionization cross section, Eq. (13), using the one-particle model potential, Eq. (14), as a function of the incident energy for

TABLE I
Parameters for the one particle model potential for different elements and their critical nuclear charges.

N (atom)	nl	δ_0	δ_1	Z_c	Z_c^a	Z_c^b
2 (He)	1s	1.066	0.881	0.912	0.91	0.92
3 (Li)	2s	0.8	0.4	2.0	2.0	2.0
9 (F)	2p	0.239	0.215	7.876	7.87	7.87

^a Critical charges from ab initio, multireference configuration interaction, computations of Hogreve [17].

^b Critical charges from Davidson's figures of isoelectronic energies [18].

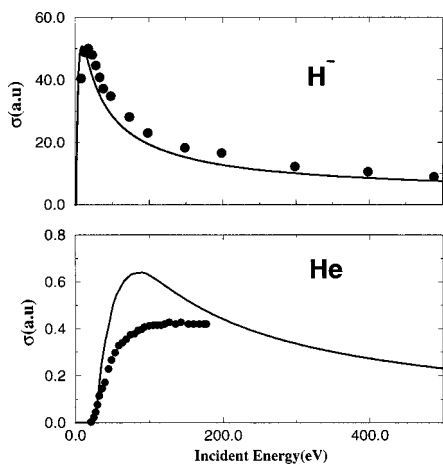


FIGURE 1. Electron impact cross section, σ , for ionization of He atom and H^- ion as a function of the electron incident energy: (—) present work; (●) experimental data are taken from Ref. [8] for He atom and Ref. [19] for H^- .

two-, three-, and nine-electron systems. Figure 1 represents a comparison between our calculated cross section and the experimental cross section for the He atom [8] and the H^- ion [19]. The parameters used for the one-electron model potential are given in Table I. This figure shows that the Born approximation gives a better agreement with the experimental cross section for the scattering of an electron from H^- than from the He atom. Figure 2 shows the same trend in comparison between the calculated cross section and the experimental re-

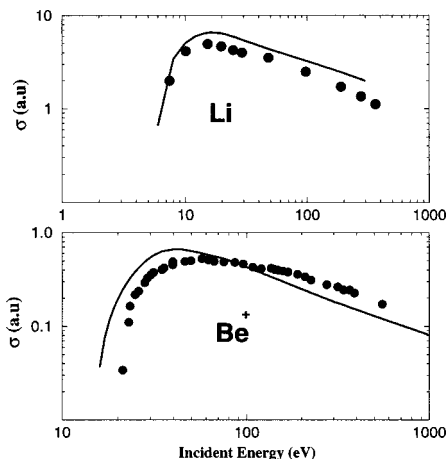


FIGURE 2. Electron impact cross section, σ , for ionization of Li atom and Be^+ as a function of the electron incident energy: (—) present work, (●) experimental data from Ref. [7].

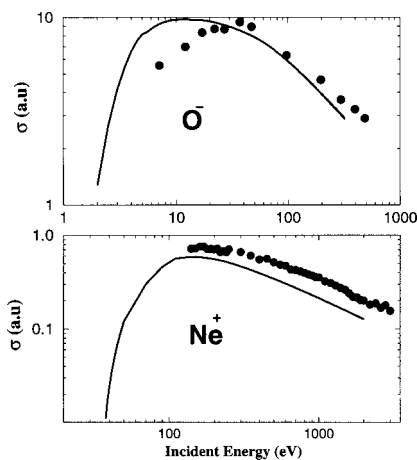


FIGURE 3. Electron impact cross section, σ , for ionization of Ne^+ atom and O^- ion as a function of the electron incident energy: (—) present work; (●) experimental data are taken from Ref. [20] for Ne^+ and Ref. [19] for O^- .

sults for three electron systems [7]. We obtain a better agreement in the case of the Li atom. Figure 3 shows the same comparison for nine-electron atoms. The cross sections for O^- is closer to the experimental data [19] than that for Ne^+ [20]. While the agreement in this case between experiment and calculation validates the approximations discussed above, we expect the Born approximation to give better results for the cross section near the critical charges (see Table I for the values of the critical charges).

The effect of varying the nuclear charge on the calculated cross section is illustrated in Figures 4, 5,

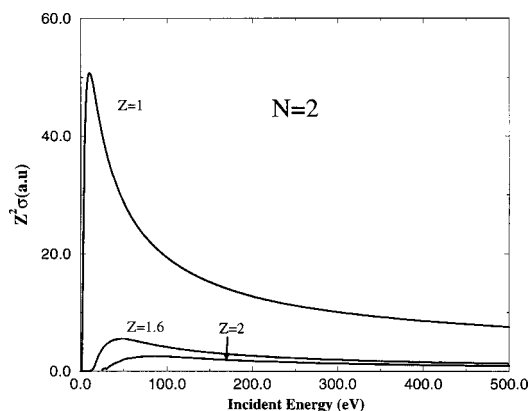


FIGURE 4. Electron impact scaled cross section, $Z^2\sigma$, for two-electron atoms, $N = 2$, as a function of the electron incident energy E for different values of the nuclear charge Z : $Z = 1$, $Z = 1.6$, and $Z = 2$.

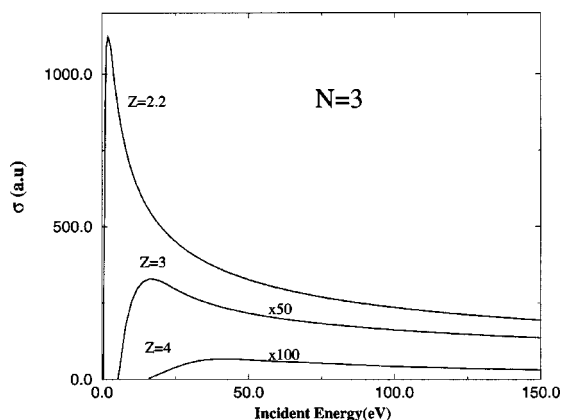


FIGURE 5. Electron impact cross section, σ , for three-electron atoms, $N = 3$, as a function of the electron incident energy E for different values of the nuclear charge Z : $Z = 2.2, 3$ (multiplied by 50 in order to put on the same scale) and $Z = 4$ (multiplied by 100).

and 6 for two, three, and nine electrons, respectively. The cross section becomes very large, for a fixed number of electrons, as one approaches the critical nuclear charge. The critical charges for $N = 2$, $N = 3$, and $N = 9$ electrons are given in Table I. Figures 7, 8, and 9 represent the cross section as a function of both the nuclear charge Z and the incident energy E . These three-dimensional plots show clearly the increase of the cross section near the critical charge Z_c .

Finally, in order to extrapolate the information to the critical charge, we plot in Figure 10 the maximum cross section as a function of the nuclear

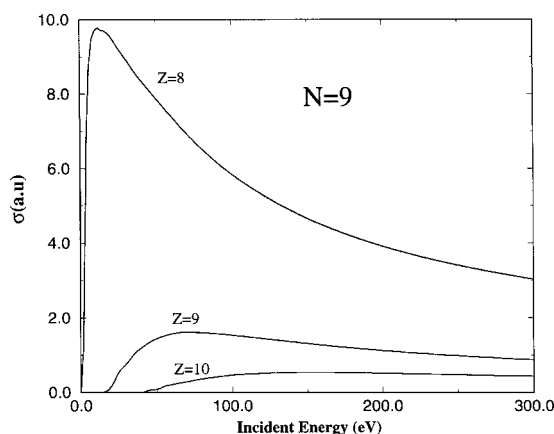


FIGURE 6. Electron impact cross section, σ , for nine-electron atoms, $N = 9$, as a function of the electron incident energy E for different values of the nuclear charge Z : $Z = 8, Z = 9$, and $Z = 10$.

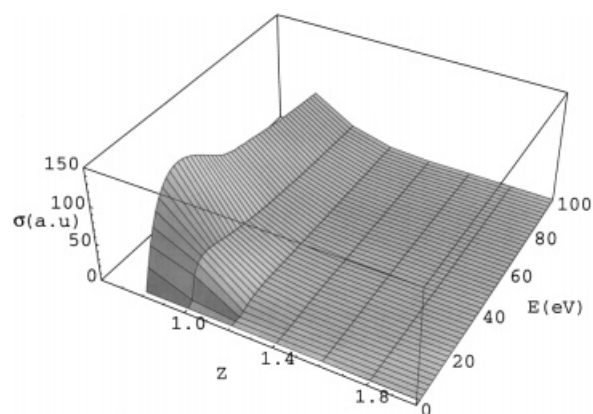


FIGURE 7. Ionization cross section, σ , for two-electron atoms as a function of both the nuclear charge Z and the electron incident energy E .

charge Z for two- and three-electron atoms. This figure shows a sharp, practically vertical, rise of the maximum cross section, σ_{\max} at the critical charges, $Z_c \simeq 0.912$, for two electron atoms $N = 2$ and $Z_c \simeq 2$ and for three electron atoms $N = 3$. Although the singularity can be well fitted to the form $\sigma_{\max} \propto (Z - Z_c)^{-3/2}$, we expect a less trivial singularity as have been established for the ionization energy $I(Z)$ for two- and three-electron atoms [21]. For two-electron atoms [1], we have shown, using the finite size scaling method, that the critical exponent for the ionization energy, $I(Z) \simeq (Z - Z_c)^\alpha$; $Z \rightarrow Z_c^+$, is equal to 1, $\alpha = 1$. For three-electron atoms [2], we obtained different results, the critical exponent was greater than 1, $\alpha \simeq 1.64 \pm 0.05$. Contrary to the helium case, where the Hamiltonian

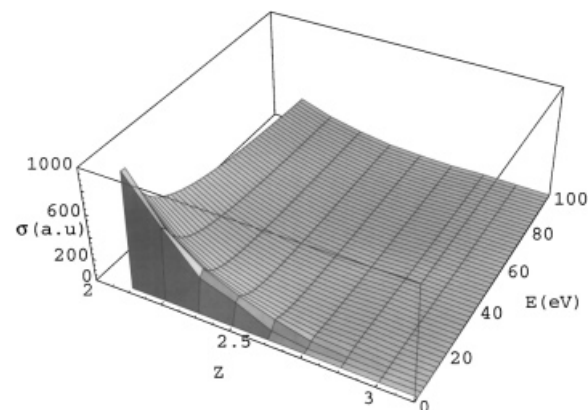


FIGURE 8. Ionization cross section, σ , for three-electron atoms as a function of both the nuclear charge Z and the electron incident energy E .

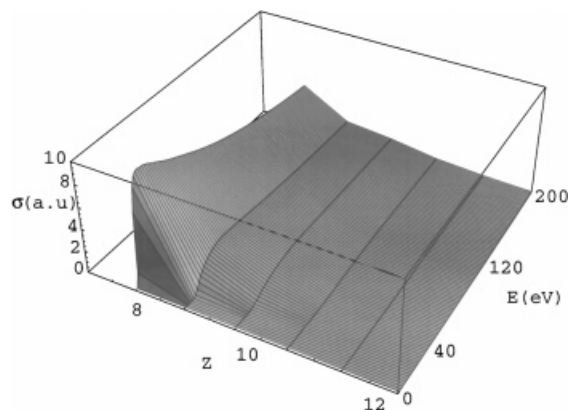


FIGURE 9. Ionization cross section, σ , for nine-electron atoms as a function of both the nuclear charge Z and the electron incident energy E .

has a square integrable eigenfunction at $Z^{(\text{He})} = Z_c^{(\text{He})}$, the Hamiltonian for lithium-like atoms does not have a square integrable wave function at the bottom of the continuum. These results show that there is a fundamental difference in behavior of the ionization energy as a function of Z for the closed-shell helium-like atoms and the open-shell lithium-like atoms. The transition in the former between a bound state to a continuum has all the characteristics of first-order phase transition while the later has a continuous phase transition. As a result of this behavior of the ionization energy near the critical Z_c , we expect the cross section to be finite for helium-like atoms and infinite for lithium-like atoms.

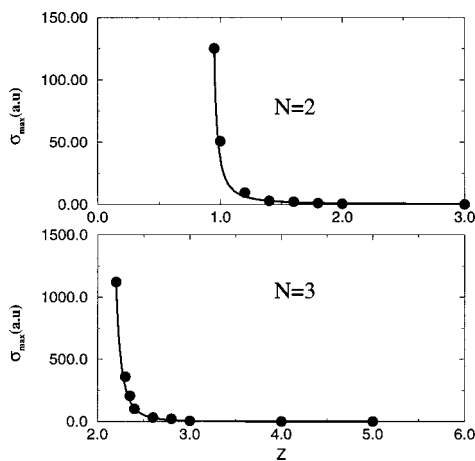


FIGURE 10. Comparison of the maximum cross section, σ_m , as a function of the nuclear charge Z for two-electron and three-electron atoms.

Conclusions

We have investigated the change of the electron impact ionization cross section as a function of the nuclear charge for two-, three-, and nine-electron atoms. We show, using the Born approximation along with a simple one-particle model, that the cross section tends to large values as the nuclear charge tends to its critical value.

In a previous study for two- and three-electron atoms, we have used the finite-size scaling method [22, 23] to study the analytical behavior of the energy near the critical point. Results for open-shell systems, such as lithium-like atoms, are completely different from those of closed-shell systems, such as the helium-like atoms. The transition in the closed-shell systems from a bound state to a continuum resemble a “first-order phase transition” while for the open-shell system, the transition of the valence electron to the continuum is a “continuous phase transition” [1, 2].

Using this analogy, we expect the analytical behavior of the cross section to be different in the cases of two-, and three-electron atoms. Since for two-electron atoms the transition is of a first order as a function of the charge, the wave function does exist and can be normalized at the critical charge Z_c . Although in our numerical calculations the cross section tends to a large value at Z_c , it must be finite. However, for the three-electron atoms, the transition is continuous and the wave function is not normalizable at the critical charge Z_c , so we expect the cross section to go to infinity at Z_c . In this study, the results for three-electron atoms show a much sharper rise in the cross section in comparison with two-electron atoms.

Although one might argue that real atoms cannot arrange their nuclear charges to be sufficiently close to the critical values, this approach might shed some light on the behavior of the cross section near singular points. Instead of taking the parameter as the nuclear charge, one can investigate this behavior as a function of external fields such as electric or magnetic fields. Research is underway to investigate the analytical behavior of the cross section as a function of external parameters.

ACKNOWLEDGMENTS

One of us (S.K.) acknowledges support of an NSF Early-Career Award.

References

1. Neirrotti, J. P.; Serra, P.; Kais, S. *Phys Rev Lett* 1997, 79, 3142.
2. Serra, P.; Neirrotti, J. P.; Kais, S. *Phys Rev Lett* 1998, 80, 5293.
3. Serra, P.; Kais, S. *Phys Rev Lett* 1996, 77, 466.
4. Serra, P.; Kais, S. *Phys Rev A* 1997, 55, 238.
5. Herschbach, D. R.; Avery, J.; Gosinski, O. *Dimensional Scaling in Chemical Physics*; Kluwer: Dordrecht, 1993; Herschbach, D. R. *Int J Quantum Chem* 1996, 57, 295, and references therein.
6. Sergeev, A. V.; Kais, S. *Int J Quantum Chem* 1999, 75, 533.
7. Bray, I. *J Phys B At Mol Opt Phys* 1995, 28, L247.
8. Raeker, A.; Bartschat, K.; Reid, R. H. G. *J Phys B At Mol Opt Phys* 1994, 27, 3129.
9. Robicheaux, F.; Wood, R. P.; Greene, C. H. *Phys Rev A* 1994, 49, 1866.
10. Andersen, L. H.; Mathur, D.; Schmidt, H. T.; Vejby Christensen, L. *Phys Rev Lett* 1995, 74, 892.
11. Pindzola, M. S. *Phys Rev A* 1996, 54, 3671.
12. Robicheaux, F. *Phys Rev Lett* 1999, 82, 707.
13. Rost, J. M. *Phys Rev Lett* 1999, 82, 1652; *J Phys B* 1995, 28, 3003; *Phys Rev Lett* 1994, 72, 1998; Rost, J. M.; Briggs, J. S. *J Phys B* 1991, 24, L393.
14. Lin, J. T.; Jiang, T. F.; Lin, C. D. *J Phys B* 1996, 29, 6175.
15. Kocbach, L. *J Phys B At Mol Opt Phys* 1976, 9, 2269.
16. Bethe, H. A.; Salpeter, E. E. *Quantum Mechanics of One- and Two-Electron Atoms*; Plenum: New York, 1977.
17. Hogreve, H. *J Phys B At Mol Opt Phys* 1998, 31, L439.
18. Charkravorty, S. J.; Davidson, E. R. *J Phys Chem* 1996, 100, 6167.
19. Tisone, G. C.; Branscomb, L. M. *Phys Rev* 1968, 170, 169.
20. Almeida, D. P.; Fontes, A. C.; Godinho, C. F. L. *J Phys B At Mol Opt Phys* 1995, 28, 3335.
21. Dubau, J.; Ivanov, I. A. *J Phys B* 1998, 31, 3335.
22. Neirrotti, J. P.; Serra, P.; Kais, S. *J Chem Phys* 1998, 108, 2765.
23. Serra, P.; Neirrotti, J. P.; Kais, S. *Phys Rev A* 1998, 57, R1481.